

Level Structure of ^{17}O from Neutron Total Cross Sections

J. L. Fowler, C. H. Johnson, and R. M. Feezel*

Oak Ridge National Laboratory,† Oak Ridge, Tennessee 37830

(Received 15 January 1973)

The neutron total cross section of oxygen is measured in the energy regions from 0.6 to 0.9, 1.12 to 1.16, and 1.39 to 4.33 MeV. More than half of this region is surveyed with energy resolution and energy steps of about 2.5 keV. On the basis of these data and supplementary published data on the (n, n) angular distributions and the $^{13}\text{C}(\alpha, n)$ reaction, the ^{17}O level energies in MeV and, in parenthesis, J^π values and center-of-mass total widths, $\Gamma_T = \Gamma_n + \Gamma_\alpha$ in keV, are: 5.696 ($\frac{1}{2}^-$, 3.4); 5.731 (not $\frac{1}{2}^+$, <1.0); 5.867 ($\frac{3}{2}^+$, 6.6); 5.937 ($\frac{1}{2}^-$, 32); 6.354 ($\frac{1}{2}^+$, 124); 6.860 (not $\frac{1}{2}^+$, <1.0); 6.970 (not $\frac{1}{2}^+$, <1.0); 7.163 ($\frac{5}{2}^-$, 1.4); 7.20 ($\frac{3}{2}^+$, 280); 7.377 ($\frac{5}{2}^+$, 0.5); 7.380 ($\frac{7}{2}^-$, 1.2); 7.56 ($\frac{3}{2}^-$, 500); 7.685 ($\frac{7}{2}^-$, 18); 7.955 ($\frac{1}{2}^+$, 90); 7.99 ($\frac{1}{2}^-$, 260); 8.058 ($\frac{3}{2}^+$, 86); 8.18 ($\frac{1}{2}^-$, 69); and 8.20 ($\frac{3}{2}^-$, 52). Resonances are not observed for known ^{17}O levels at 5.215 and 7.573 MeV; these levels have $\Gamma_T < 0.1$ keV. The previously reported narrow $\frac{3}{2}^+$ level at 7.694 MeV does not exist. Many of the results are based on a multilevel R -matrix analysis; this is also extended to the published $^{16}\text{O}(n, n)$ and $^{13}\text{C}(\alpha, n)$ cross sections for energies corresponding to ^{17}O excitations up to 9.5 MeV. This extension shows that there are two levels rather than only one near 8.47 MeV and that the 9.42-MeV level has $J^\pi = \frac{3}{2}^-$. Other assignments are confirmed. The most accurate excitation energies below 9.5 MeV are reviewed from the literature and the ^{17}O - ^{17}F mirror structure is reviewed.

I. INTRODUCTION

The mass-17 nuclei ^{17}O and ^{17}F have relatively simple level structures which have been studied, both theoretically and experimentally, for many years. Recently, several shell-model calculations were reviewed by Lemaire, Mermaz, and Seth.¹ Experimentally, much information is available. A few years ago one could say² that the data were more complete for ^{17}F than for ^{17}O . That situation is now reversed. The 1971 review by Ajzenberg-Selove,³ which includes some of the present results, lists almost 50 reactions that have contributed to the experimental structure of ^{17}O . Since that review at least two more papers have appeared; Lemaire, Mermaz, and Seth¹ studied many levels by the $^{15}\text{N}(^3\text{He}, p)^{17}\text{O}$ reaction and Baker *et al.*⁴ measured neutron polarization from $^{13}\text{C}(\alpha, n)$. These many experiments contain data not only on the energies and J^π values but also on the structures of the states.

The present paper on neutron total cross sections is a member of a series.^{2,5,6} Here we report total cross sections measured with good statistics, good energy resolution, and accurate energies over most of the neutron energy region below 4.3 MeV. We then analyze the data over a broad energy region by the multilevel two-channel R -matrix theory.⁷ A companion paper⁸ gives most of the analysis and the interpretation in terms of spectroscopic factors, and this paper gives details of the individual resonances. With the help of the earlier neutron-scattering angular distributions^{2,6} and $^{13}\text{C}(\alpha, n)$ data,⁹⁻¹⁴ we assign the J^π , Γ_T , and resonant energies for most of the observed levels.

We also review the total-cross-section data of Fossan *et al.*¹⁵ for energies from 4.3 to 5.8 MeV and, with the help of the $^{13}\text{C}(\alpha, n)$ data, assign or confirm some J^π values in that region.

The measurements are discussed in Sec. II and the individual resonances in Sec. III. A tabulation of the data from these sections is available from the National Neutron Cross Section Center at the Brookhaven National Laboratory. In Sec. IV, we reanalyze some earlier angular distributions² in light of the present results. In Sec. V we summarize the level assignments and review the most accurate energies for the known levels below 9.5 MeV in ^{17}O , and in Sec. VI we compare these with those in ^{17}F .

II. MEASUREMENTS OF σ_T

The $^7\text{Li}(p, n)^7\text{Be}$ and $^3\text{H}(p, n)^3\text{He}$ reactions are complementary neutron sources. The first reaction in a thin lithium target yields neutrons with good resolution, but it has a second neutron group because the residual ^7Be nucleus can be left in its 430-keV excited state. The second reaction in a tritium-gas target has no second group, but the entrance foil introduces large energy spreads and uncertainties in the neutron energies. So, we use the $^7\text{Li}(p, n)$ reaction with corrections for the second group for our precision energy measurements with high resolution and use the $^3\text{H}(p, n)$ source to check the cross sections at off-resonance energies.

A. Transmission Geometry

We measure the total cross section much as discussed previously² by observing the transmission

of a BeO sample relative to a matching Be sample for neutrons produced in one or the other of these (p, n) reactions by analyzed protons from the Oak Ridge National Laboratory's 5.5-MV electrostatic accelerator. The scattering sample is held in a light-weight support at 0° midway between the source and the detector, which is a 2.5-cm-diam stilbene crystal with associated electronics for pulse-shape discrimination against γ rays. At each energy an automatic system interchanges the scatterers in the four-step sequence, Be-BeO-Be-BeO, in which each step is terminated and the data recorded after a predetermined number of monitor counts.

The source-to-detector distance is 41 to 47 cm except for a few points near some narrow resonances, where it is 32 cm. We use Wick's limit for 0° differential cross sections in making the inscattering correction for most of the points. A few cross checks by use of the actual 0° values^{2,6} show this correction to be good to 0.01 b. The correction is less than 2% except at the peaks of some resonances. Near resonances we analyze in detail, we use the observed^{2,6} cross sections at 0° .

In order to correct for the background from the room, we compare at a few energies the counts with the Be scatterer with those with the detector shielded by a 30-cm-long truncated cone of Lucite and make a small correction for transmission of the Lucite. For the ${}^7\text{Li}(p, n)$ source the corrections to the total cross sections average about 3% and never exceed 6%; for the ${}^3\text{H}(p, n)$ source, they are about half as large.

B. Measurements and Results with the ${}^3\text{H}(p, n)$ Source

The tritium target is a 1-cm-atm cell¹⁶ with a Ni entrance foil. In order to measure the effective foil thickness we observe ${}^{16}\text{O}(n, n)$ resonances, the energies of which we know from accurate data taken with the ${}^7\text{Li}(p, n)$ source. The neutron energy spread, as evidenced by the widths of the resonances, is 30 keV full width at half maximum and is due mostly to the nonuniformities in the foil; the proton energy loss in the gas is only 12 to 20 keV.

Figure 1 shows the cross sections measured with this source. The size of each point is about equal to the uncertainty arising from counting statistics, and the error symbols, which are shown on a few representative points and are scarcely larger than the points, are derived by combining the statistical uncertainties in quadrature with one third of the corrections for background and inward scattering. The smooth curve is the multilevel R -matrix fit⁸ smeared by a 30-keV Gaussian resolution function.

C. Techniques for the ${}^7\text{Li}(p, n)$ Source

This section is devoted to the thin targets and precision energies, which are aspects of the high-resolution measurements, and to the corrections for the second neutron group, which must be made to obtain cross sections.

1. Thin Lithium Targets

The preparation and maintenance of thin Li targets are crucial to our high-resolution work. Figure 2 illustrates the target assembly. The target backing is soldered onto a 6.7-cm-long brass tube which is the Faraday cup. To deposit the lithium, we transfer the cup to a position above a lithium-filled boat in an evacuated bell jar. A shield prevents the deposition of impurities while the lithium temperature is raised to the evaporating point. We make the evaporation and then transfer the target in an argon-filled plastic bag to the assembly, which is standing by filled with helium. During the subsequent evacuation, the target is isolated from organic vapors by liquid-nitrogen traps in both the assembly and the roughing line. An external air-water jet cools the target, which is oscillated by its coupling through the flexible brass bellows to an eccentric drive¹⁷ during the proton bombardment. With this arrangement we have used 8- μA proton beams for about 100 h with negligible target deterioration.

The backing material is important. We started with Pt but found that the target deteriorates as the

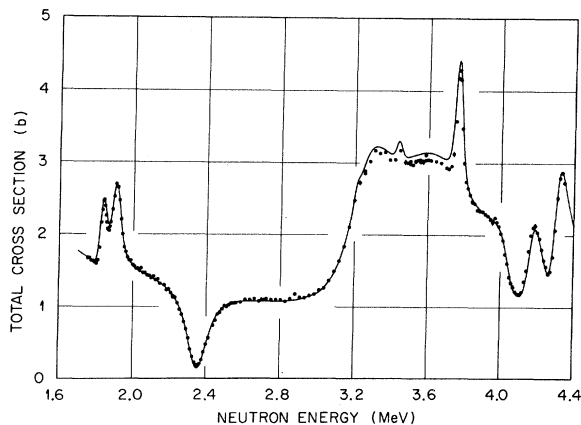


FIG. 1. The total cross section of oxygen for neutrons produced with a 30-keV energy spread from the ${}^3\text{H}(p, n)$ reaction. The energy scale is chosen to make the resonant energies agree with those in Fig. 3. The statistical uncertainties are less than the heights of the symbols and the total uncertainties are about the same or slightly larger than the symbols. The curve is calculated by the multilevel two-channel R -matrix theory and folded into a 30-keV Gaussian resolution function.

lithium diffuses into the platinum. Macklin¹⁸ had found that diffusion is negligible for W or Ni. We used tungsten for our differential cross-section measurements⁶ and for some of the present work. Unfortunately, tungsten blisters after about 100 μAh of bombardment apparently because hydrogen pressure builds up inside the metal. A nickel backing does not blister but has other disadvantages. At the higher energies the background from (p, n) reactions in natural Ni is appreciable. We used natural Ni for a few low-energy points but soon changed to enriched ^{58}Ni , an isotope with the (p, n) threshold above our energy region. A backing of ^{58}Ni evaporated as a thin protective layer onto 0.01-cm Pt proved to be very stable and provided us with most of our high-resolution data, but eventually it ruptured and allowed the lithium to diffuse into the platinum. Finally, we had ^{58}Ni rolled into a solid 0.01-cm-thick backing and had the outside plated with gold to prevent corrosion by the air-water cooling jet. Targets on this backing were stable, but the Ni eventually fractured from heating by the beam. At present, we believe that a backing of 0.03-cm ^{58}Ni is most promising for a very stable target.

Extraneous neutrons come not only from the backing of natural Ni but also from some impur-

ity in the backing of ^{58}Ni . To obtain data to correct for these neutrons, we wash off the Li and measure the yields and transmissions for neutrons from the backing at a few energies. The corrections to σ_T are usually less than $\pm 1\%$.

2. Accurate Neutron Energies

The energies that we report for resonances with $\Gamma < 20$ keV represent averages from several observations, often taken months apart, with random errors less than ± 1 keV and usually about ± 0.5 keV. Essentially, the accuracy with which a neutron resonant energy can be determined depends on the measurement of the difference between the average relativistic proton energy in the target at the resonance and the proton energy at the true ^7Li - (p, n) threshold. To measure this difference we use a proton magnetic resonance probe in the analyzing magnet. Magnetic saturation causes the average field to rise less rapidly than the field at the probe. For our magnet a correction curve has been determined primarily by measuring the neutron yields near standard (p, n) thresholds and by finding the intercepts from linear extrapolations as discussed by Beckner *et al.*¹⁹ The energy uncertainty introduced into our measurements, aside

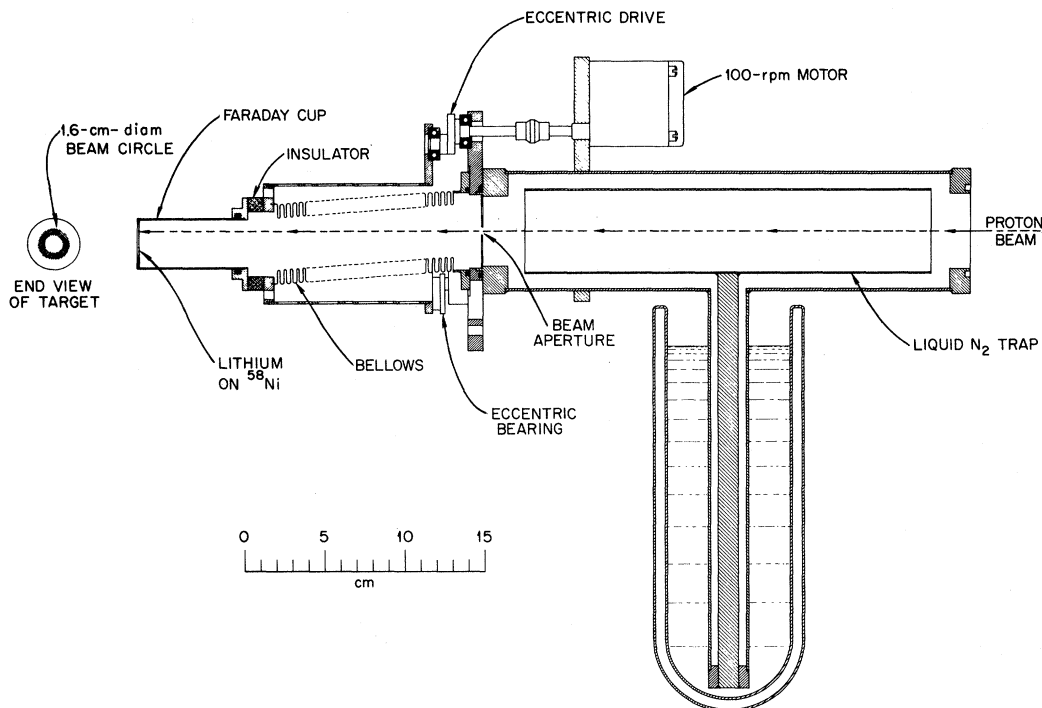


FIG. 2. The lithium target assembly. The target is prepared by evaporation and transferred to this assembly. Beam damage to the target is minimized by the presence of the cold trap, by oscillation of the target, and by maintenance of an external air-water cooling jet. The nickel backing prevents deterioration by diffusion of the Li into the backing. The ^{58}Ni isotope is used because it has a high (p, n) threshold.

from the uncertainties in the standards themselves, is ± 0.5 keV. The curve is based mostly on the threshold energies^{20,21} for targets of ^3H , ^7Li , ^{19}F , and ^{27}Al . Also, the shape for higher fields has been determined¹⁴ from observations of the relative flux-meter settings for bending singly- and doubly-charged α particles of the same energy; three $^{19}\text{F}(\alpha, n)$ resonances were observed in thick targets in order to give relative calibration points equivalent to about 2.5- and 10-MeV protons. The curve which we use is a two-parameter expression that fits exactly the threshold energies for ^3H , ^7Li , and ^{19}F and gives an $^{27}\text{Al}(p, n)$ threshold of 5798.3 keV in agreement with Marion's²¹ weighted average of 5796.9 ± 3.8 keV. Since the $^7\text{Li}(p, n)$ threshold has a negligible uncertainty (± 0.07 keV) and the error in the $^{19}\text{F}(p, n)$ threshold is small (± 0.8 keV), the uncertainties for neutron energies below 2.5 MeV are less than ± 0.8 keV. The larger uncer-

tainty in the $^{27}\text{Al}(p, n)$ threshold propagates to our measurements with an uncertainty which increases with energy, up to ± 3.8 keV for 4.2-MeV neutrons.

In regard to the true $^7\text{Li}(p, n)$ threshold, Newson *et al.*²² showed that experimental conditions can displace the experimental value, as determined from a straight-line intercept, either above or below the true value. For our work the ~ 1 -keV proton-beam resolution and the ~ 3 -keV target thickness at threshold both tend to shift the experimental value about 0.3 keV, but the effects tend to cancel.²² We assume that the experimental and true thresholds occur at the same energy with an uncertainty of ± 0.3 keV.

The average proton energy at a resonance is less than the incident energy by half of the loss in the target. Our over-all resolution, as determined from observed widths of narrow resonances, is due mostly to the target thickness rather than to

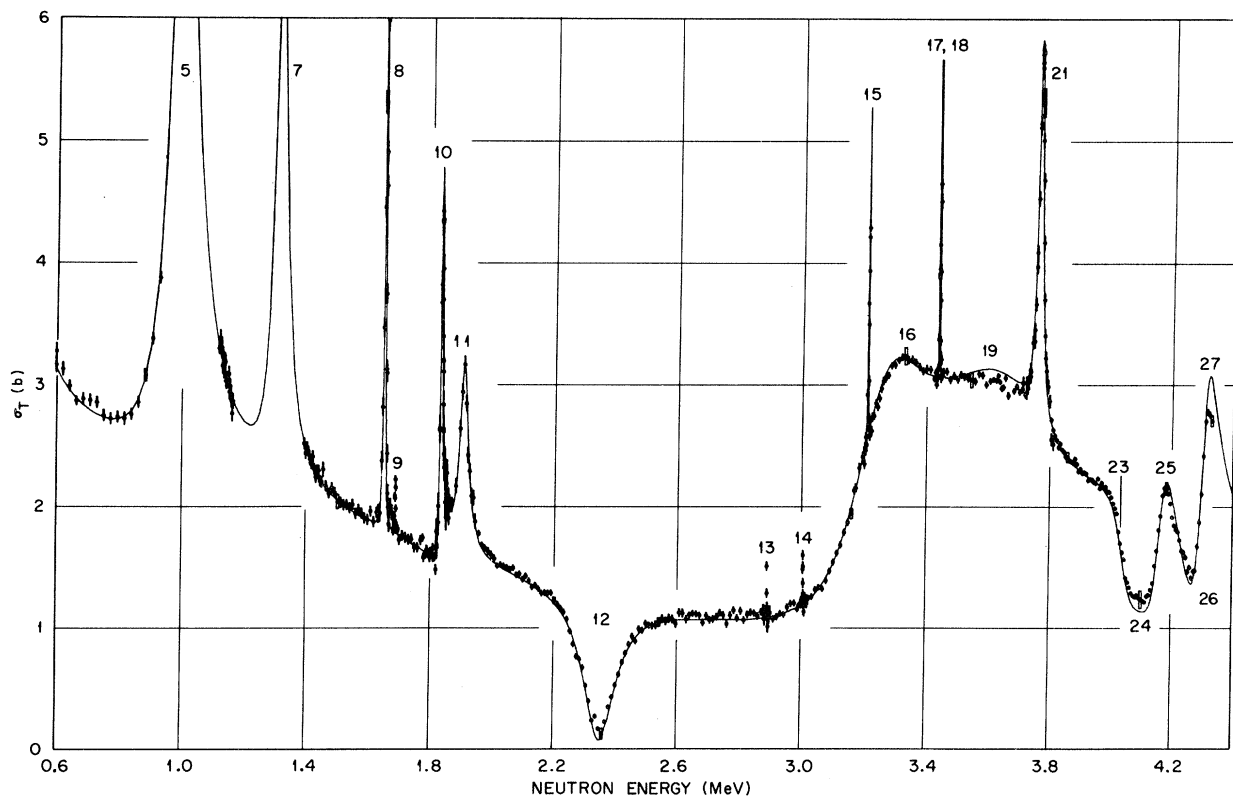


FIG. 3. The neutron total cross section for oxygen measured with good resolution with the $^7\text{Li}(p, n)$ source. The resonance numbers refer to ^{17}O levels in Table III and the smooth curve is a multilevel R -matrix fit without corrections for finite resolution. Most of the resonances are shown on expanded scales in Figs. 4–8. Most of the data were obtained with energy resolution and energy spacings of about 2.5 keV and are shown averaged over regions of 6 to 10 keV except near narrow resonances. The vertical heights of the symbols represent the statistical uncertainties. The vertical bars for some representative data points show the total absolute uncertainties. These bars are scarcely visible below 3 MeV. Corrections have been applied for the second neutron group. Comparisons with Fig. 1 show the errors in the correction are negligible except from 3.3 to 3.5 MeV and near 4.1 MeV, where the points here are about 0.06 b too high, and at the 4.3-MeV peak, where they are about 0.25 b too low.

the spread in the incident proton energy. So we assume target thicknesses of slightly less than the resolution widths and make appropriate corrections for the variation of stopping power with energy. For the region studied with high resolution, this correction has an uncertainty of ± 0.3 keV.

We calculate the neutron energy at the average angle subtended by the 2.5-cm-diam detector; this energy is 0.2 keV less than at 0° . To quote total uncertainties we first combine in quadrature the above errors related to the true threshold, target thickness, calibration standards, and random errors in the magnet curve and in the observed resonances. Then we round these upwards to the nearest keV and also round the energies themselves to the nearest keV.

3. Second Neutron Group from $^7\text{Li}(p, n)$

To correct the transmissions for the second neutron group in the $^7\text{Li}(p, n)$ reaction we need to know the relative abundances, detector efficiencies, and total neutron cross sections for both groups.

A curve derived from published data^{19, 23, 24} and plotted versus the energy of the primary group shows that the abundance of the second group relative to the first rises from zero at 0.65 MeV to a broad peak of 12.5% at 2.3 MeV, decreases to 9% at 3.3 MeV, and finally rises to about 32% at 4.3 MeV. These percentages are modified slightly for the transmission measurements because of the shielding effects of the Be nuclei for the two groups; hence, the Be total cross sections²⁵ enter into the corrections.

The ^{16}O total cross sections at the energies of the two groups are available both from the literature and from our present work. In order to use our data, we make an iteration to find the final cross sections required for self-consistent corrections.

The measurement of relative efficiencies requires an auxiliary experiment in which the scintillator and a long counter are placed symmetrically to the beam axis. We compare the counting rates as a function of the primary neutron energy, make a small correction for the detection of the second group by the scintillator, and determine the scintillator's response function under the assumption that the long counter is flat over the 0.45-MeV interval corresponding to the separation of the groups. For the transmission measurements the bias settings are such as to give higher efficiencies for the primary group.

We made several sets of measurements with various Li targets over a period of many months and obtained the total cross sections for oxygen throughout the energy regions from 600 to 900, 1116 to 1162, and 1390 to 4330 keV. About 60%

of these data were obtained during searches for narrow resonances using 2- to 3-keV resolution for the energies, 1116–1162, 1633–1697, 1821–1851, 1954–3669, and 3712–3811 keV. Within these regions we normally used steps of about 2.5 keV but sometimes smaller steps. For the remaining 40% of the total region our resolution was about 5 to 10 keV and, in particular, above 3811 keV it varied from 4 to 8 keV even though the steps were kept to 3 keV.

The results are shown in Fig. 3 and, for most of the resonances, on expanded energy scales in other figures in Sec. III. The resonances are marked with level numbers for ^{17}O as tabulated in Sec. V. To reduce the statistical scatter of points we have averaged the cross sections over spans of 6 to 10 keV except near the sharp resonances. In averaging, each datum point is used only once. An earlier technical report²⁶ shows the data from 1.8 to 3.65 MeV on an expanded energy scale.

The heights of the symbols for most of the points represent the uncertainties from counting statistics. A few points are shown as solid vertical bars to represent the total estimated uncertainty obtained by combining the statistics in quadrature with one third of each of the corrections for background, in-scattering neutrons from the second group.

The only significant absolute uncertainties in the cross sections arise from the second-group corrections. These errors can be evaluated by comparisons with the $^3\text{H}(p, n)$ data in Fig. 1. The R -matrix curve, which is shown without energy averaging in Fig. 3, is a useful vehicle for the comparison. (A more direct comparison is given in a preliminary report.²⁷) The corrections that have been applied are generally very good and, except at the 4.3-MeV peak, always better than ± 0.1 b. The agreement at the 2.35-MeV minimum is significant because there the correction for the second group is $\sim 50\%$. There are small but definite discrepancies near 3.4, 4.1, 4.2, and 4.3 MeV. From 3.3 to 3.5 MeV the cross sections obtained with the $^7\text{Li}(p, n)$ source are about 2% or 0.06 b too high, indicating that the applied correction of 5% is too large. This error obscures the broad 3.6-MeV peak which is clearly established by the $^3\text{H}(p, n)$ data. At the 4.1-MeV minimum the $^7\text{Li}(p, n)$ points are about 0.07 b too high, indicating that the correction of -17% should be more negative, and at 4.21 MeV a faint inflection for the $^7\text{Li}(p, n)$ data is caused by an overcorrection for scattering of the second group, which happens to have the energy of the 3766-keV resonance. The most serious error occurs for the three highest energy points near the 4.3-MeV peak. These points average 2.76 b whereas the R -matrix curve, which agrees with

the ${}^3\text{H}(p, n)$ data, averages 3.04 b. It appears that correction for the second group should be increased from the value used (3%) to approximately 10%. This may be due to a resonance for production of the second group at this energy.²⁴ (Other errors could be present in these three points; they were obtained near the upper limit for the accelerator and were not verified by repeat measurements.)

Except for the effects of resolution and the errors for the second group, the present results agree well with those by Fossan *et al.*¹⁵ In particular their measurements with a tritium target also show that the 4.1-MeV minimum should be deeper than observed here with the lithium target and that the 4.3-MeV peak should be higher. In general, the present results agree, except for resolution effects, with the time-of-flight data of Cierjacks *et al.*,²⁸ although their cross sections are systematically ~ 0.05 b higher than ours for 2.6- and 3.1-MeV neutrons.

III. RESONANCES IN σ_T

The smooth R -matrix curves in Figs. 1 and 3 are calculated with parameters chosen to fit not only the present data but also the total cross sections from Wisconsin^{15, 29-31} for energies up to 5.8 MeV and the (n, α) cross sections from this laboratory.¹⁴ The details of specific resonances are given here but most of the R -matrix analysis and the interpretation are in the companion paper.⁸ Table I and the following subsections, A-C, list the resonances that are observed here; those searched for but not observed; the J^π values derived either directly or with the aid of data from the literature; and the resonant energies and total widths, E_r and Γ_r , either from the multilevel analysis of overlapping resonances or from equivalent single-level analyses of the isolated peaks. Data shown are those from the ${}^7\text{Li}(p, n)$ source. The resonant energies and widths in Table I supersede the values

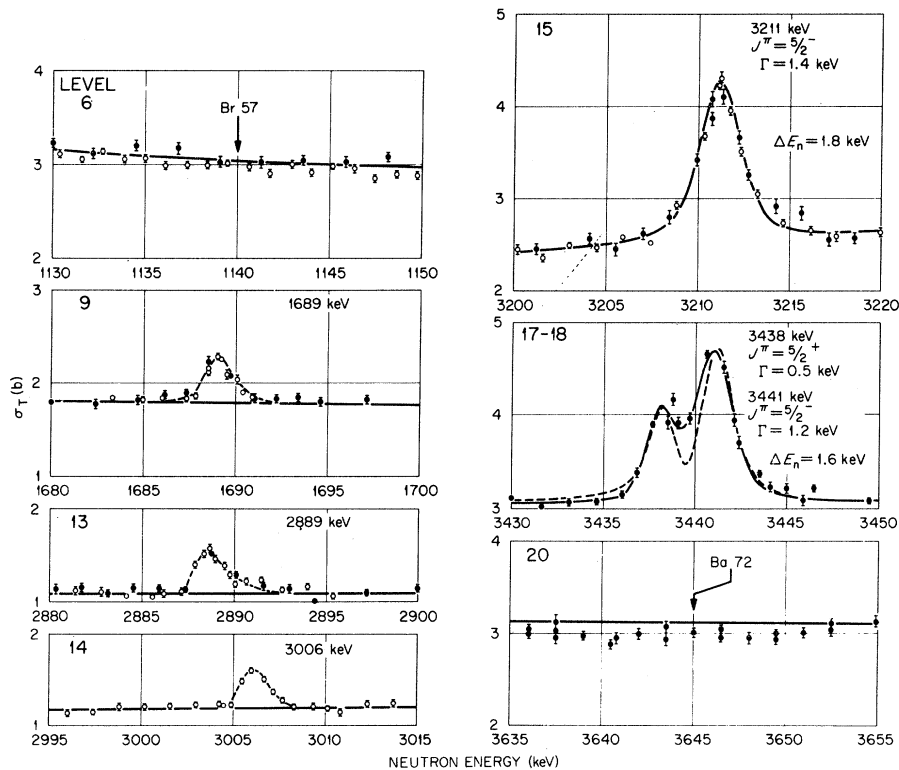


FIG. 4. Total cross sections for energies near eight narrow levels in ${}^{17}\text{O}$. The level numbers are from Table III. For level 6 the arrow corresponds to the 5.215 MeV excitation reported in Ref. 33. For level 20 the arrow is deduced from the ${}^{13}\text{C}(\alpha, n)$ data of Ref. 14. These two states must have $\Gamma < 0.1$ keV. The other six resonant energies are each averages for at least two measurements in the present work. Open and closed circles represent different sets of data. The narrow resonances for levels 9, 13, and 14 have $\Gamma < 1.0$ keV. The solid curves show the R -matrix fit. The resonant curves for levels 15, 17, and 18 are the equivalent single-level resonances with parameters as indicated and averaged for Gaussian resolution functions of the indicated widths. The dashed curve for levels 17 and 18 is calculated assuming two $\frac{5}{2}^-$ resonances.

in our earlier papers.^{6,32} Section IIID lists similar results deduced by the analysis of measurements above 4.3 MeV by other workers.^{14, 15, 31} Multilevel definitions of the single-level quantities, E_r and $\Gamma_T = \Gamma_n + \Gamma_\alpha$, are in the companion paper [see Eqs. (13) and (22)]. All widths are in the laboratory system unless specifically indicated as center of mass. The level numbers refer to a tabulation for ^{17}O in Sec. V.

A. Narrow Levels 6, 9, 13-15,
17-18, and 20

Our cross sections near these eight levels are shown in Fig. 4. Six resonances are observed with $\Gamma < 2$ keV. Four of these had not been seen before in the total cross sections and the other two, being only 3 keV apart, had been reported¹⁵ as a single peak. The solid points represent data obtained with one target and the open circles with another one several months later. The resonant energies listed in the figure and in Table I are based on averages from these and repeat measurements. In the figure we have applied small energy shifts so that the peaks for these particular data occur at the average energies. The peak at 3006 keV is an example of a resonance that we could have missed in the broad-range survey; although our first scan²⁶ with 2.5-keV steps revealed the 2889-keV peak, it did not reveal this one. The points show a later search³² which we made because other reactions³ had indicated a level near here.

The solid curves are from the broad-range R -matrix fit.⁸ They give good fits to the nonresonant cross sections except near 3.65 MeV where the curve is about 0.1 b high. Only three of the levels had been studied sufficiently in other reactions to be included with known J^π values in the R matrix. The solid curves for these three are folded into Gaussian resolution functions of the indicated widths.

Although levels 6 and 20 are known³ from other reactions, our high-resolution search did not reveal them. The arrow for level 6 corresponds to Browne's³³ excitation energy of 5215 keV. This arrow is surely close to the right place because Browne's energies for other sharp unbound levels (8, 9, and 10) agree with ours to ± 1 keV. For level 20 the arrow corresponds to the energy reported by Bair and Haas¹⁴ except that it is broken and displaced downward by 2 keV because our energies for nearby levels 15, 17, and 18 are also displaced about 2 keV from theirs. We estimate $\Gamma < 0.1$ keV for each of these levels.

The small peaks for levels 9, 13, and 14 each have a height of less than half of that predicted for $J = \frac{1}{2}$; hence, for each one, the observed width of

≤ 2 keV is essentially the resolution width, and $\Gamma < 1$ keV. These levels cannot have $J^\pi = \frac{1}{2}^+$ because resonances for s waves would interfere with the large potential scattering to give dips rather than peaks. This unambiguous conclusion is pertinent to the ^{17}O - ^{17}F mirror levels (see Sec. VI).

For level 15 the observed 2.7-keV width includes some broadening from the natural width. We can fit this resonance with either $J = \frac{5}{2}$ or $\frac{7}{2}$ using resolution widths consistent with the preceding narrower peaks; however, the $^{13}\text{C}(\alpha, n)$ angular distribu-

TABLE I. Resonant parameters from present measurements. Resonant energies and widths supersede values of Refs. 6 and 32.

^{17}O level	J^π	E_r (lab) (MeV \pm keV)	Γ_T (cm) ^a (keV)
6 ^b		1.140 ^b	<0.1
8	$\frac{7}{2}^-$	1.651 \pm 2	3.4
9 ^c	not $\frac{1}{2}^+$	1.689 \pm 2	<1
10	$\frac{3}{2}^+$	1.833 \pm 2	6.6
11	$\frac{1}{2}^-$	1.908 \pm 4	32
12	$\frac{1}{2}^+$	2.351 \pm 8	124
13 ^c	not $\frac{1}{2}^+$	2.889 \pm 2	<1
14 ^c	not $\frac{1}{2}^+$	3.006 \pm 2	<1
15 ^c	$\frac{5}{2}^-$ ^d	3.211 \pm 3	1.3
16	$\frac{3}{2}^+$	3.25 \pm 10	280
17	$\frac{5}{2}^+$ ^d	3.438 \pm 3	0.5
18	$\frac{5}{2}^-$ ^d	3.441 \pm 3	1.1
19	$\frac{3}{2}^-$	3.63 \pm 20	500
20 ^b		3.647 ^b	<0.1
21	$\frac{7}{2}^-$	3.766 \pm 4	18
23	$\frac{1}{2}^+$	4.053 \pm 8	90
24	$\frac{1}{2}^-$	4.09 \pm 50	270
25	$\frac{3}{2}^+$	4.162 \pm 8	85
26 ^{c, e}	$\frac{1}{2}^-$ ^f	4.29 \pm 20	69
27	$\frac{3}{2}^-$ ^f	4.31 \pm 10	52 ^g

^a Uncertainties in widths about $0.1\Gamma_T$ for $\Gamma_T > 3$ keV and about $0.3\Gamma_T$ for $\Gamma_T < 3$ keV.

^b Known levels searched for but not found in total cross section.

^c Narrow levels not previously detected in total cross section.

^d Assignment based in part on $^{13}\text{C}(\alpha, n)$ and $^{16}\text{O}(n, n)$ angular distributions, Refs. 6, 9, 11, and $^{13}\text{C}(\alpha, n)$ data from Ref. 14.

^e Level first reported here.

^f Assignment based in part on $^{13}\text{C}(\alpha, n)$ distribution, Ref. 11.

^g Deduced, in part, from data in Ref. 15.

tions^{9, 11} require $J = \frac{5}{2}$. Also odd parity is required to fit the neutron differential scattering.⁶ Using this assignment, $\frac{5}{2}^-$, we fit the peak as shown in the figure.

To assign J^π values for the doublet levels 17 and 18 we need also the data from three other sources, those^{6, 11} with poor energy resolution for the $^{16}\text{O}(n, n)$ and $^{13}\text{C}(\alpha, n)$ angular distributions, and those with good resolution for the angle-integrated $^{13}\text{C}(\alpha, n)$ yields.¹⁴ The present data rule out $\frac{1}{2}^+$, $\frac{3}{2}^-$, or $\frac{3}{2}^+$ because these assignments give interference minima rather than peaks. Also $\frac{1}{2}^-$ is ruled out by the observed height of the upper peak and of the lower shoulder. (The shoulder was reproduced in repeat measurements.) Thus, $J > \frac{3}{2}$ for both members. However, both members cannot have the same J^π because interference would then give a deeper minimum than observed between the peaks. In Fig. 4 this is illustrated by the dashed curve which is calculated for $J^\pi = \frac{5}{2}^-$ with resonant widths and energy resolution to fit the upper and lower sides of the doublet. Turning to the $^{13}\text{C}(\alpha, n)$ reaction, the absence of P_6 and higher Legendre polynomials for the angular distributions¹¹ for the unresolved doublet shows that $J < \frac{7}{2}$ for the lower member, which contributes 70% of the yield,¹⁴ but does not rule out $J > \frac{5}{2}$ for the upper weaker member. Finally, given $J = \frac{5}{2}$ for the lower member, the neutron scattering distributions obtained⁶ with ~5-keV resolution at energies near the upper peak can be fitted only with $J^\pi = \frac{5}{2}^-$ for this peak under the conditions that the nonresonant phase shifts be consistent with those at nearby energies and that the widths be consistent with the total cross sections. Since the levels must have different J^π , our

final assignment is $\frac{5}{2}^+$ for level 17 and $\frac{5}{2}^-$ for level 18. The solid curve is calculated with the indicated parameters. The energy resolution is consistent with the observed widths of the other narrow levels. The off-resonant curve shows slightly lower cross sections at energies below the doublet than it does above because of interference with the negative $d_{5/2}$ phase shifts. The fact that the data points are also slightly higher gives additional support to $\frac{5}{2}^+$ for one member of the doublet.

B. Levels 8, 10-12, and 21

We find a resonant energy of 1651 ± 2 keV for level 8 from measurements with several different targets. Lane *et al.*³⁴ found from the distribution of the scattered neutrons that the resonance is due to f waves, and they assigned $J^\pi = \frac{7}{2}^-$ rather than $\frac{5}{2}^-$. We attempted to make this selection absolute by showing that the peak total cross section is well above the maximum for $J = \frac{5}{2}$. Figure 5 shows our run with the highest peak or best resolution. The scatterer had 0.1686 atoms/b, and the data have been corrected for in-scattering of f waves. Since the observed maximum is 0.3 b more than allowed for $J = \frac{5}{2}$, we assign $J > \frac{5}{2}$. We rule out even parity because the observed width of the resonance corresponds to about 10 times the single-particle width for g waves. Thus, we assign $J = \frac{7}{2}^-$ in agreement with Lane *et al.* The figure shows the R -matrix curve, or the identical Breit-Wigner resonance, folded into a Gaussian resolution function. The widths, $\Gamma_{\text{lab}} = 3.6$ keV and $\Delta E_n = 2.4$ keV, are chosen to give the observed height and width. Recent higher-resolution measurements³⁵ by time of flight at this laboratory confirm the Γ derived here and show definitely that $J > \frac{5}{2}$.

For levels 10 and 11 we find resonant energies of 1833 ± 2 and 1908 ± 4 keV as shown in Fig. 6. To measure the lower peak we used the same target as in Fig. 5 but for the upper peak we used 5-keV resolution. The curve is the R -matrix fit folded into Gaussian resolution functions of one or the other widths, and it is equivalent to that obtained by the single-level formula with $\Gamma = 7$ keV for level 10, $\Gamma = 34$ keV for level 11, and with potential phase shifts of -11° for $d_{3/2}$ and -0.3° for $p_{1/2}$. The fact that three points with good statistics near 1.97 MeV lie above the curve suggests that the $p_{1/2}$ potential phase shift is about -5° rather than nearly zero. Not only are the E_r , Γ_T , and J values for these two resonances established by the energies, widths, and heights of the peaks but also the parities are revealed by the peak shapes. As reported years ago³⁶ the 1908-keV resonance must result from p waves rather than s waves because it is a peak rather than a dip. For the 1833-keV reso-

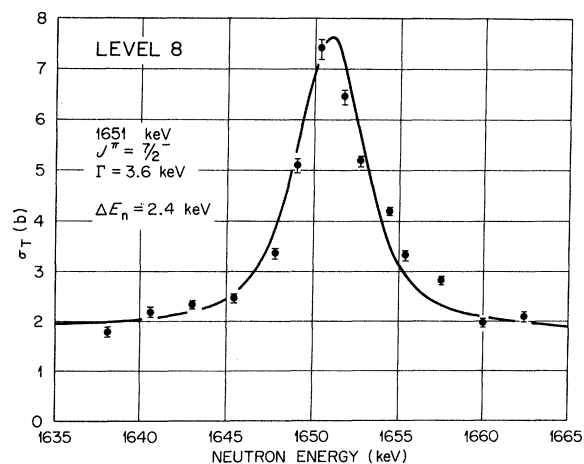


FIG. 5. Neutron total cross section near level 8 in ^{17}O . The resonant curve is calculated for either a single or multilevel formula and folded into a Gaussian resolution function with parameters as indicated. The nonresonant contributions are from the multilevel analysis.

nance, the minimum which precedes the peak requires interference with $d_{3/2}$ waves if it is to be consistent with the broad-range R -matrix analysis; this confirms the $\frac{3}{2}^+$ assignment from scattering measurements.⁶

The s -wave minimum corresponding to *level 12* is well known.³⁶ We find the minimum of 0.13 b^{27} at $2353 \pm 8 \text{ keV}$ and $\Gamma_T = 132 \text{ keV}$. The R -matrix analysis gives a resonant energy of 2351 keV .

Figure 7 shows the resonance for *level 21*. The resonant energy of $3766 \pm 4 \text{ keV}$ agrees with $3765 \pm 3 \text{ keV}$ by Davis and Noda.³¹ The resolution width of 2.4 keV , much less than the observed width, is deduced from an observation of the narrow 3211-keV peak. To make the inward-scattering correction we use the 0° cross sections for f waves rather than Wick's limit. At the peak the points with two different bias settings provide a cross check on the correction for the second group, which can be large at these energies. For the solid points the bias was such as to make the correction 10% of the height of the peak above the nonresonant background; for the open circle the correction was 4.5%. The peak height shows that $J = \frac{7}{2}$, and the large width of 19 keV suggests strongly that $J = \frac{7}{2}^-$, rather than $\frac{7}{2}^+$, in agreement with the angular distributions.^{2,37} The curve in the figure is calculated, with corrections for energy resolution, from parameters that are the same as for the broad-range R -matrix fit except that the $d_{3/2}$ phase shifts here are made 2° less negative in order to fit the off-resonant cross sections. The $f_{7/2}$ potential phase shift is 2° but the fit would improve slightly if it were zero; certainly this potential phase shift must be small. The literature contains errors

about this level. The peak total cross section from both our earlier work² and from Fossan *et al.*¹⁵ seemed to show $J = \frac{5}{2}$, in contradiction to $\frac{7}{2}^-$ from the angular distributions. To remove this discrepancy we earlier proposed² an additional $\frac{3}{2}^+$, 3.772-MeV resonance. That level should now be deleted from the literature.³ In retrospect, our earlier resolution must have been worse than we thought; perhaps there was diffusion of the tritium out of the thin zirconium film into the target backing. The earlier angular distributions are reanalyzed in Sec. IV.

C. Overlapping Levels 16, 19, 23-27, and also 28

Except for levels 17, 18, and 21, as discussed above, the resonances between 3 and 4.4 MeV are overlapping and require the multilevel analysis.

The very broad $\frac{3}{2}^+$ and $\frac{3}{2}^-$ resonances, *levels 16 and 19*, near 3.3 and 3.65 MeV are well known from differential scattering measurements,^{2,37,38} but the corresponding total-cross-section peaks have not been discussed previously. The 3.3-MeV peak is clearly visible in both Figs. 1 and 3 but the 3.65-MeV peak is obvious only in Fig. 1. Both peaks were seen in the time-of-flight measurements of Cierjacks *et al.*²⁸ The resonant energies and total widths from the multilevel analysis⁸ are given in Table I.

The resonant structure above 3.8 MeV is more complicated. In fact, the reason for extending the analysis to the higher-energy total cross sections from Wisconsin^{15,31} and to the (n, α) cross sections,¹⁴ particularly the cluster of resonances up to 5.3 MeV , is to understand this region. In Fig. 8

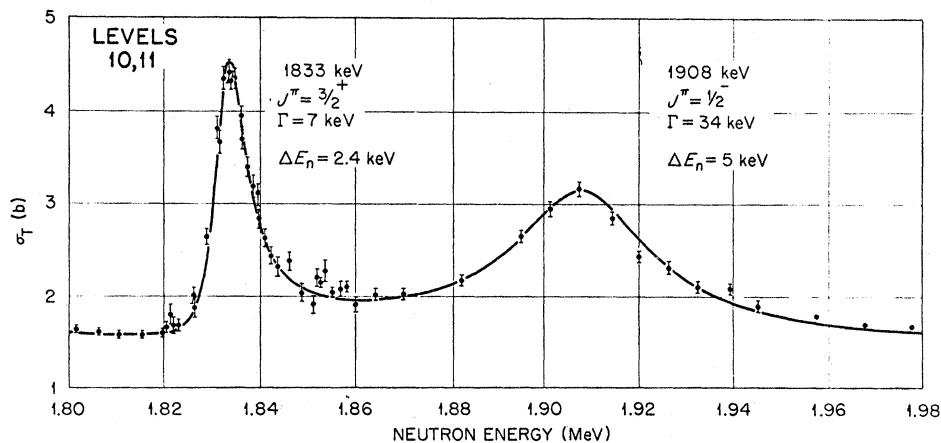


FIG. 6. Neutron total cross sections near levels 10 and 11 in ^{17}O . The points near level 10 were measured with the same 2.4-keV target as in Fig. 5 but the points near level 11 were measured with a 5-keV target. The three points above 1.95 MeV are from a third set of data. The solid curve is the multilevel fit, or the equivalent single-level curve, folded into Gaussian resolution functions of one or the other widths.

the upper figure shows the R -matrix fit to both the total and the angle-integrated (n, α) cross sections from 3.8 to 4.5 MeV. The larger circles are the present data from Fig. 3; the caption gives the references of the other data. As stated above, the present data would fall nearer to the curve at 4.1, 4.2, and 4.32 MeV if a better correction were made for the second group from the ${}^7\text{Li}(p, n)$ source. The lower figure shows the total cross sections for the four dominant partial waves. The resonances, one each for $\frac{3}{2}^+$ and $\frac{3}{2}^-$ and two each for $\frac{1}{2}^+$ and $\frac{1}{2}^-$, correspond to levels 23 through 28 in ${}^{17}\text{O}$. (Our own data do not include level 28.)

Prior to this analysis it was believed³ that there were only the four levels that are clearly visible in both the total and (n, α) cross sections. We are convinced that the assignments for six levels in the figure are uniquely required to fit $\sigma_{n, \alpha}$ and σ_T ; nevertheless, we cannot argue easily without the aid of additional angular-distribution data. For the following argument we accept only a minimum of additional data, namely, that P_2 is the highest even-order polynomial needed to fit the distributions observed¹⁰⁻¹² in the inverse ${}^{13}\text{C}(\alpha, n){}^{16}\text{O}$ reaction. Thus, $J < \frac{5}{2}$ for all levels. Also there must be consistency with the observed σ_T and $\sigma_{n, \alpha}$ both above and below this narrow region.

The argument, based on extensive efforts to fit the data by the R -matrix theory, is as follows: The four obvious resonances for levels 23, 25, 27, and 28 occur at about 4.05, 4.17, 4.31, and 4.47 MeV. Our assignment of $\frac{1}{2}^+$ to the first and last of these is unambiguous; the slight maximum followed by a minimum in σ_T for each one is characteristic of a large positive potential phase shift, which is supplied only by s waves in this region. Also, this assignment of s waves for the 4.05-MeV anomaly

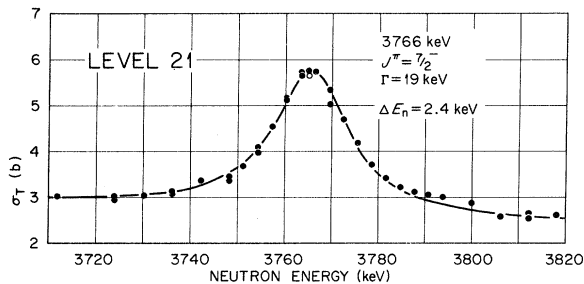


FIG. 7. Total cross section near the resonance for level 21 in ${}^{17}\text{O}$. The solid points were obtained with a 10% correction for the presence of the second group at the peak, and the open circle was obtained with a 4.5% correction. The solid curve is obtained by folding a Gaussian resolution function into a single-level resonance which is equivalent to the multilevel curve except that the absolute magnitude of the $d_{3/2}$ phase shift has been reduced by 2° here to improve the off-resonant fit.

in σ_T yields the observed energy for the (n, α) peak. The magnitude of the 4.17-MeV peak in σ_T requires $J = \frac{3}{2}$. The 4.31-MeV peak height would require $J = \frac{5}{2}$ for a single resonance but, since the (α, n) angular distributions demand $J < \frac{5}{2}$, it requires two resonances of which at least one has $J = \frac{3}{2}$. These resonances for $J = \frac{3}{2}$, one at 4.17 MeV and the other at 4.31 MeV, have opposite parity because the valley in σ_T between the peaks is too shallow for interference between levels of the same parity. Near 4.1 MeV, since the $\frac{1}{2}^+$, $\frac{3}{2}^+$, and $\frac{3}{2}^-$ curves are all near their minima, there must be a broad $\frac{1}{2}^-$ resonance, level 24, to fill in the observed cross sections. The parities can now be established as $\frac{3}{2}^+$ and $\frac{3}{2}^-$, respectively, for the 4.17- and 4.31-MeV resonances because there must be continuity with the broad $\frac{3}{2}^+$ and $\frac{3}{2}^-$ peaks at 3.3 and 3.65 MeV. (If the parities were reversed but σ_T were still fitted near 4.1 MeV, the cross sections near 3.65 MeV would be much too high.) This completes the assignments for all but the second state, level 26, underlying the 4.31-MeV peak. Only the additional $\frac{1}{2}^-$ resonances will fit both this

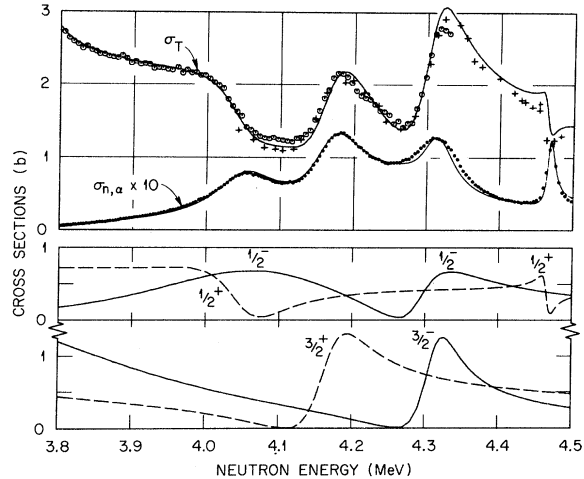


FIG. 8. Neutron total and angle-integrated (n, α) cross sections for resonances for the six ${}^{17}\text{O}$ levels, 23-28, which the analysis shows to have $J^\pi = \frac{1}{2}^+$, $\frac{1}{2}^-$, $\frac{3}{2}^+$, $\frac{3}{2}^-$, $\frac{3}{2}^-$, and $\frac{1}{2}^+$, respectively. The (n, α) cross sections are derived from the ${}^{13}\text{C}(\alpha, n)$ data of Ref. 14 and normalized by a factor of 0.8 (in addition to the indicated plotting factor of 10). For the total cross sections, the crosses are from Ref. 15 and the circles are the present data for the ${}^7\text{Li}(p, n)$ source. The corrections applied for the second group were relatively large and a comparison with Fig. 1 shows that the open circles should fall nearer to the solid curve at 4.1 and 4.2 MeV and at the 4.31-MeV peak. The curves are the R -matrix fit. Partial total cross sections are shown in the lower figures, and the partial (n, α) cross sections are in the companion paper, Ref. 8.

peak and the preceding valley in σ_T . Thus, we complete the J^π assignments for levels 23–28.

The foregoing argument makes little use of the fact that the $\sigma_{n,\alpha}$ data are also fitted. As a matter of interest we released the requirement of $J < \frac{5}{2}$ imposed by the (α, n) angular distributions and allowed the 4.31-MeV resonance to be single with $J^\pi = \frac{5}{2}^+$. Then σ_T can be fitted fairly well, but not $\sigma_{n,\alpha}$. This result and others obtained with various level assignments lead us to believe that our final assignments are uniquely required to fit the data in Fig. 8.

The fact that the two underlying $\frac{1}{2}^-$ levels 24 and 26 are not immediately visible from the data accounts for the confusion that has existed in this region even though it has been studied extensively, not only in σ_T and $\sigma_{n,\alpha}$, but also by neutron differential scattering,^{2,37} by both polarization^{39,40} and differential yields^{10–12} from the $^{13}\text{C}(\alpha, n)$ reaction, and by other reactions.³ The other four resonances for levels 23, 25, 27, and 28 are particularly visible in the (n, α) reaction and the J values assigned here agree with those^{10,11} from early $^{13}\text{C}(\alpha, n)$ angular distributions. However, those early distributions seemed to show alternating parities for the trio (23, 25, and 27). Thus, when neutron-differential-scattering measurements^{2,37} led to the $\frac{3}{2}^+$ assignment for the central member (25), which we confirm, these three levels were assumed to be $\frac{1}{2}^-$, $\frac{3}{2}^+$, and $\frac{3}{2}^-$. This erroneous $\frac{1}{2}^-$ assignment for the lower member seemed to be confirmed by the scattering measurements^{2,37} which showed a broad $\frac{1}{2}^-$ resonance in this region. But this is level 24. The other underlying $\frac{1}{2}^-$ resonance for level 26 has not been previously reported. Both scattering measurements missed the $\frac{1}{2}^+$ resonance for level 23. A reanalysis of our earlier angular distributions² is presented in Sec. IV.

D. Levels 28, 30, 31, 33, 34, and 41 from the Data of Other Workers

Parameters for these levels are summarized in Table II. As stated above, the analysis in the companion paper extends to the measurements of other workers for 4.4- to 5.8-MeV neutrons. The J values and relative parities for most of the levels in ^{17}O corresponding to these neutron energies have been reported from $^{13}\text{C}(\alpha, n)$ angular distributions.^{10–13} Absolute parities cannot be determined^{40,41} from that reaction, either by angular distributions or polarization studies, but can be found from either $^{16}\text{O}(n, n)$ or $^{13}\text{C}(\alpha, \alpha)$ elastic scattering. Barnes, Belote, and Risser¹² and Kerr, Morris, and Risser¹³ made absolute-parity assignments by first measuring the (α, α) scattering for resonances where this process dominates

and then, having determined the absolute parity of these few levels, assigned the rest relative to them. Since a wrong assignment could propagate to several wrong ones, it is important to obtain cross checks from (n, n) scattering.

The unambiguous $\frac{1}{2}^+$ assignment for level 28, as discussed above, agrees with that of Barnes, Belote, and Risser.¹² This is supportive evidence for their values for other nearby levels.

In regard to levels 30 and 31 in Table II, it is obvious without a detailed analysis that the level associated with the 4.61-MeV resonance in σ_T is not the same one that gives rise to a resonance in $^{13}\text{C}(\alpha, \alpha)$ scattering at a corresponding α -particle energy. Barnes, Belote, and Risser¹² observed the (α, α) -scattering resonance and found $J^\pi = \frac{7}{2}^+$. We designate this as level 30. It must have $\Gamma_\alpha \gg \Gamma_n$. A small resonance in (α, n) is observed at the same energy. A resonance in σ_T corresponding to level 30 would have to have $\sigma_T \leq 0.1$ b. Fosson *et al.*¹⁵ observed a resonance with $\sigma_T \geq 0.46$ at ~ 4.61 MeV, and they assigned $J \geq \frac{3}{2}$. This cannot be level 30; we designate it as 31. Barnes *et al.* assumed that the resonance in (α, n) results from the same level (30) that gives rise to the strong (α, α) scattering. They then based the parity of the nearby states on the absolute parity of level 30. If the (α, n) yield should happen to be associated with the other level (31) their assignments for the nearby states could be wrong. It is important to find confirmation from the (n, n) scattering.

Confirmation is provided by the multilevel analysis.⁸ For levels 33, 34, and 41, which correspond to neutron resonances at 4.83, 5.05, and 5.61 MeV, the observed¹⁵ peaks in σ_T require $J = \frac{3}{2}$. The interference (Fig. 12 of Ref. 8) in the angle-integrated (n, α) cross sections¹⁴ shows that the central member (level 34) has $J^\pi = \frac{3}{2}^+$ just as level 25. The absence of interference minima in σ_T between the resonances for 33, 34, and 41 shows that the parities alternate, i.e., $\frac{3}{2}^-$, $\frac{3}{2}^+$, $\frac{3}{2}^-$. The first two of these are confirmations of the work of Barnes, Belote, and Risser¹²; the latter is a new assignment.

Polarization studies of the (α, n) reaction by Baker *et al.*⁴ give some hint of the upper $\frac{3}{2}^-$ state and possibly for the lower $\frac{1}{2}^-$ levels 24 and 26.

IV. ANGULAR DISTRIBUTIONS

Various workers^{2, 5, 6, 29, 37, 38, 42} have measured the scattering distributions for 0.4- to 4.7-MeV neutrons on ^{16}O . Below 2.15 MeV the s , p , and $d_{3/2}$ phase shifts deduced by Fowler and Cohn⁵ are in essential agreement ($\pm 5^\circ$) with the present R -matrix analysis; perhaps a minor exception is that

their curves suggest that the $d_{3/2}$ phase shift vanishes or is negative below 0.8 MeV, whereas the present curve is slightly positive, e.g., $+4^\circ$ at 700 keV. Above 3 MeV the analyses of Johnson and Fowler² and of Lister and Sayres³⁷ are in essential agreement, but neither reveals the s -wave resonance near 4.05 MeV. It is important to find out whether both of those analyses actually contradict the existence of the s -wave resonance or simply have the wrong minima. (Such searches can encounter false minima.)

As a first step, let us assume that the s -wave curve deduced here, as shown in Fig. 9 from 2.75 to 4.25 MeV, is correct. This assumption should be very good below 3 MeV where the s -wave scattering is dominant. Above 3 MeV the extrapolation of the nonresonant part on the basis of the diffuse-edge potential should be fairly good. As discussed above, the 4.05-MeV s -wave resonance is based on the detailed fit to both the total and (n, α) cross sections. Let us also assume the f -wave phase shifts, which are generally small, are given by the R -matrix analysis.⁸ The p - and d -wave curves from the R -matrix analysis are shown in Fig. 9, and the data points are obtained by searching only on the four p - and d -wave phase shifts to fit the distributions from Figs. 3, 4, and 6 of Johnson and Fowler.² The agreement of the points with the curves shows that those earlier distributions are consistent with the R -matrix analysis and, specifically, with the 4.05-MeV s -wave resonance. The $d_{5/2}$ points are interesting; the off-resonant average of -6.9° agrees well with the corresponding average of -5.4° from the R -matrix curve. It seems that the angular distributions are quite sensitive to the small $d_{5/2}$ phase shift. [Points above 3.9 MeV in Fig. 10 are not quite right because the (n, α) channel has been neglected, but the error is small because the (n, α) cross sections are small.]

If we now continue the search by including the s -wave phase shift as a fifth variable, we can go

monotonically to a deeper minimum in each case; however, for some of the distributions, the new p - and d -wave phase shifts are not continuous with those at adjacent energies. In such cases, we can visualize the search as following a long gentle valley in which slight changes for s waves require drastic changes for other partial waves. Our conclusion is that the uncertainties in the angular distributions are sometimes too large to define all five phase shifts and, particularly, to determine those for both $p_{1/2}$ and $s_{1/2}$. It seems not too surprising that both earlier phase-shift analyses^{2, 37} missed the s -wave resonance.

As stated in Sec. III B, since the previously reported cross section at the 3.766-MeV peak was too small for a single $\frac{7}{2}^-$ resonance, the scattering distributions near the resonance were analyzed earlier² under the wrong assumption of an additional narrow $\frac{3}{2}^+$ state. Figure 10 shows a reanalysis for a single resonance with $J^\pi = \frac{7}{2}^-$, $\Gamma = 19$ keV. For distributions A, B, and C we followed the above procedure by fixing the s - and f -wave phase shifts at the R -matrix values and then searching on the four p - and d -wave phases. The three sets of phases are in mutual agreement and the average values, which are designated by arrows in Fig. 9, are consistent with the R -matrix curves. The fits improve slightly if the s -wave phase is also varied. However, for distribution D any search on both p -wave phases yields $p_{1/2}$ and $p_{3/2}$ shifts inconsistent with the off-resonant values; in this case we have fixed $p_{3/2}$ rather than $s_{1/2}$ at the R -matrix value. (We expect little uncertainty for $p_{3/2}$ waves because this is not far from the broad 3.65-MeV peak where the $p_{3/2}$ phase shift must be 90° .) The fit for D is not as good as for the other three but the phase shifts are consistent with the off-resonant values. This difficulty may be associated with the neutron energy spectrum²; a Gaussian energy spectrum was assumed but the actual spectrum is unknown.

TABLE II. Level assignments from present analysis of data on σ_T by Fossan *et al.* (Ref. 15) and on $\sigma_{n, \alpha}$ by Bair and Haas (Ref. 14).

Level in ^{17}O	E_r (lab) (MeV)	Present analysis	Barnes, Belote, and Risser (Ref. 12)	Fossan <i>et al.</i> (Ref. 15)
28	4.47	$\frac{1}{2}^+$	$\frac{1}{2}^+$...
30	4.60	not same level	$\frac{7}{2}^+$...
31	4.61		...	$\geq \frac{3}{2}$
33	4.83	$\frac{3}{2}^-$	$\frac{3}{2}^-$	$\frac{3}{2}$
34	5.05	$\frac{3}{2}^+$	$\frac{3}{2}^+$...
41	5.61	$\frac{3}{2}^-$...	$\geq \frac{3}{2}$

TABLE III. Accurate and recommended ^{17}O excitation energies. An asterisk denotes a measurement fitted by resonant energy in the R -matrix analysis of Ref. 8.

Level	$2J^\pi$ ^a	Γ_T (c.m.) ^b (keV)	Recommended energy (MeV)	$^{16}\text{O}(n,n)$ ^c (MeV \pm keV)	$^{16}\text{O}(d,p)$ ^d (MeV \pm keV)	
0	5 ⁺		0	($Q=4.1426$) ^e		
1	1 ⁺		0.8708 ^f		0.871 \pm 4	
2	1 ⁻		3.055		3.055 \pm 4	
3	5 ⁻		3.846		3.846 \pm 5	
4	3 ^{-g}	45 ^h	4.550	4.550 \pm 2 ⁱ	4.553 \pm 6	
5	3 ⁺ ^g	96 ^h	5.083	*5.083 \pm 2 ¹	5.083 \pm 10	
6	7 \rightarrow 11 ^j	<0.1	5.215		5.215 \pm 5	
7	3 ^{-g}	42 ^h	5.377	*5.377 \pm 2 ¹	5.378 \pm 7	
8	7 ^{-g}	3.4	5.696	*5.696 \pm 2	5.695 \pm 5	
9	Not 1 ⁺ ^k	<1.0	5.731	5.731 \pm 2	5.731 \pm 5	
10	3 ⁺ ^g	6.6	5.867	*5.867 \pm 2	5.866 \pm 5	
11	1 ^{-g}	32	5.937	*5.937 \pm 4	5.940 \pm 15	
12	1 ⁺ ^g	124	6.354	*6.354 \pm 8		
13	Not 1 ⁺ ^k	<1.0	6.860	6.860 \pm 2		
14	Not 1 ⁺ ^k	<1.0	6.970	6.970 \pm 2		
15	5 ⁻¹	1.3	7.164	*7.163 \pm 3	7.165 \pm 2	7.168 \pm 5
16	3 ⁺ ^g	280	7.20	*7.20 \pm 10		
17	5 ⁺ ¹	0.5	7.378	*7.377 \pm 3	7.379 \pm 2	7.380 \pm 5
18	5 ⁻¹	1.1	7.381	*7.380 \pm 3	7.382 \pm 2	
19	3 ^{-g}	500	7.56	*7.56 \pm 20		
20	≥ 7 ^m	<0.1	7.573		7.573 \pm 2	7.573 \pm 5
21	7 ⁻¹	18	7.685	*7.685 \pm 4	7.691 \pm 6	7.684 \pm 5
22	(11 ⁻)		7.76 ⁿ			
23	1 ⁺ ^k	90	7.952	7.955 \pm 8	*7.950 \pm 8	
24	1 ^{-k}	270	7.99	*7.99 \pm 50		
25	3 ⁺ ^g	85	8.060	8.058 \pm 8	*8.062 \pm 8	
26	1 ⁻¹	69	8.18	*8.18 \pm 20		
27	3 ^{-g}	52	8.197	8.20 \pm 10	*8.197 \pm 8	
28	1 ⁺ ^g	12 ^h	8.347		*8.347 \pm 4	8.347 \pm 5
29	5 ⁺	5 ^h	8.403		*8.406 \pm 3	8.402 \pm 5
30	7 ⁺	8 ^h	8.468		*8.471 \pm 3	8.467 \pm 5
31	≥ 3 ^o	≤ 11 ^o	8.48	8.48 ± 10 ^o		
32	5 ⁻	5 ^h	8.501		*8.505 \pm 3	8.502 \pm 5
33	3 ^{-g}	44 ^h	8.685		*8.689 \pm 5	8.498 ± 3 ^p
34	3 ⁺ ^g	78 ^h	8.892		*8.897 \pm 8	
35	7 ⁻	6 ^q	8.90 ^q			
36	7 ⁻	25 ^h	8.963	8.961 ± 4 ^r	*8.969 ± 4	See Ref. 13
37	1 ⁻	7 ^s	9.140		9.144 ± 4	9.144 ± 5
38	(9 ⁻)		9.16 ⁿ			
39	7 ⁻	3 ^q	9.18 ^q			
40	5 ⁺	7 ^s	9.195		9.197 ± 4	9.200 ± 5
41	3 ^{-o}	120 ^h	9.42	*9.42 ± 10 ^o		
42	5 ⁻	15 ^s	9.485		9.489 ± 4	9.496 ± 5

^a The J^π values not indicated otherwise are from the review of Ref. 3.

^b Widths not otherwise indicated are from Table I of the present measurements.

^c Neutron-resonant energies not otherwise indicated are from present measurements.

^d See Ref. 33.

^e C. Maples, G. W. Goth, and J. Cerny, Nucl. Data 2, 429 (1966).

^f See Ref. 43.

^g Previously assigned J^π values confirmed by present R -matrix analysis.

^h Widths based on the work of others and presented in the companion paper (Ref. 8).

ⁱ Reference 35 and unpublished data by same authors.

^j F. A. Rose, Nucl. Phys. A124, 305 (1969).

^k Present measurement and analysis.

^l Assignment from R -matrix analysis based in part on present measurement.

^m See Ref. 11.

ⁿ See Ref. 1.

^o R -matrix analysis of data from Refs. 15 and 31.

^p R. M. Williamson, T. Katman, and B. S. Burton, Phys. Rev. 117, 1325 (1960).

^q Energies and widths based on $^{13}\text{C}(\alpha, \alpha)$ data in Refs. 12 and 13.

^r See Ref. 31.

^s Width is average from Refs. 13 and 14.

V. ACCURATE LEVEL ENERGIES FOR ^{17}O

Although the levels below 9.5 MeV in ^{17}O have been studied in many reactions^{4,3} and all but a few of the levels have been observed in at least two reactions, the energies have been measured accurately and with good resolution (~ 5 keV) in only a few experiments. Table III lists the energies and uncertainties from the high-resolution measurements.

Let us discuss these data in order of increasing energy. The first excited state is known⁴⁸ to within ± 0.2 keV from γ -ray measurements. This state is also included in Browne's³³ measurements of the $^{16}\text{O}(d, p)^{17}\text{O}$ reaction to the first 11 excited states. Above 4 MeV excitation Browne's measurements overlap the accurate energies from the neutron total cross sections, and the excellent

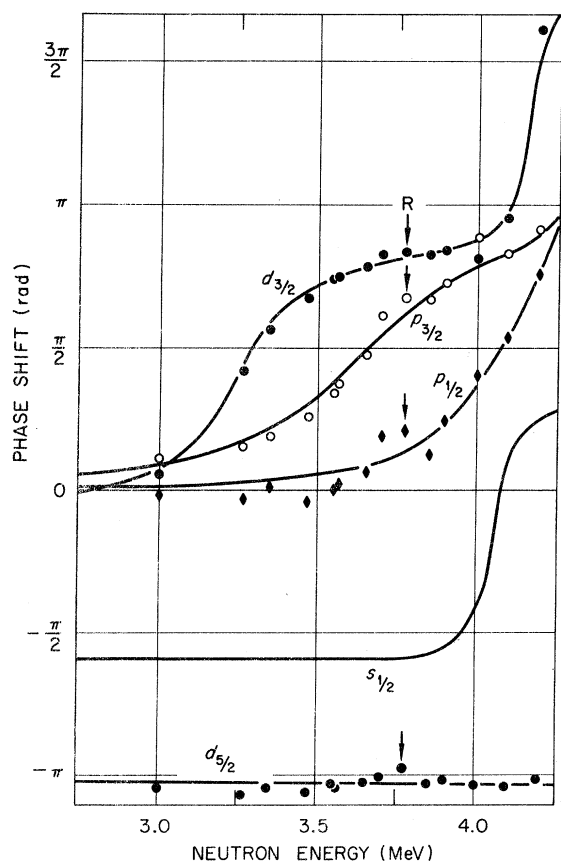


FIG. 9. Phase shifts for least-squares fits to the neutron scattering distributions from Ref. 2. The curves are from the present R -matrix analysis and the points are from searches in which only four p - and d -wave phases are varied while the s and f waves remain fixed at the R -matrix values. Points indicated by arrows near the 3.766-MeV resonance are averages from the first three distributions in Fig. 10.

agreement indicates that his quoted uncertainties are too conservative. For the $^{16}\text{O}(n, n)$ scattering the first three entries (levels 4, 5, and 7) are from recent unpublished³⁵ studies by time of flight with 5-nsec neutron bursts and a 198.73-m flight path. The next $^{16}\text{O}(n, n)$ energies, up through level 27, are from the present measurements; the last three (31, 36, and 41) are derived from the Wisconsin data.^{15,31} Above 7 MeV excitation these data overlap those from the $^{13}\text{C}(\alpha, n)$ reaction for which several studies have been published³ but only the values reported with good resolution are included in the last two columns of the table.

The table includes level energies that we recommend on the basis of these data. For levels 1–21 the bases are obvious from the table, but various criteria are used for the higher levels. For level 23 and above, the $^{13}\text{C}(\alpha, n)$ resonant energies are recommended, providing the level is observed by the reaction, except that we have shifted the higher levels systematically downward a few keV to force better agreement with the accurate value reported³¹ from neutron total cross sections for level 36. The accuracy for this resonance and others at higher energies has been confirmed by recent time-of-flight measurements.³⁵ Since (α, n) resonances are not observed for levels 31 and 41, the less accurate total cross-section energies are recommended.

Four other levels have been reported only in other processes. For levels 22 and 38, which are high-spin states observed^{4,3} in multiparticle reactions, we adopt the energies which Lemaire, Mermaz, and Seth¹ obtained with 30-keV resolution because their energies for other levels agree well with those in the table. The final two levels, 35 and 39, have been clearly resolved only in $^{13}\text{C}(\alpha, \alpha)$ scattering. Barnes, Belote, and Risser¹² reported the lower one (35) at 8.884 MeV but we have shifted it to 8.90 MeV in order to bring about a consistency in the table with the other nearby levels reported by Barnes *et al.* The energy for level 39 comes from the same experiment¹³ as for the last three energies in the last column of the table.

An asterisk denotes an energy that is fitted in the present multilevel analysis. These energies may not correspond to the maxima in the (n, α) or (n, n) cross sections for broad or overlapping resonances; the resonant and peak energies are listed in the companion paper.⁸

The J^π values are from the tabulation of Ajzenberg-Selove unless otherwise indicated. Over half of these are made or confirmed by the present analysis. For level 20 the $\frac{7}{2}^-$ assignment derived³⁹ with very poor resolution is not included. Lemaire, Mermaz, and Seth¹ present theoretical specula-

tions for most of the levels (6, 9, 13, 14, 20, 22, and 38) for which J^π values are not yet measured.

The total c.m. widths are also listed in the table. About half of these are from Table I above. The others are based on data from the literature.

All but levels 16, 19, 24, 26, 31, 41, 35, and 39 have been clearly observed in more than one process. Of these eight, the first six have been observed only in neutron elastic scattering and the latter two in $^{13}\text{C}(\alpha, \alpha)$ scattering. Some indications of these levels might have been found in other studies.^{3, 4}

VI. ^{17}O - ^{17}F MIRROR LEVELS

Figure 11 shows the known levels in ^{17}O and ^{17}F up to 9.5 MeV. The ^{17}O level numbers, energies, and J^π values are from Table III. The ^{17}F values are from Table 17.17 of Ajzenberg-Selove's review³ except for a new⁴⁴ level at 5.215 MeV and modified⁴⁵ J^π values for levels 29, 30, and 31.

We have attempted to clarify the picture by separating the scheme into two parts with the definite mirrors to the left and the remaining levels to the

right. Our criteria for a definite pair are conservative. We require that both J^π values be measured, that the nucleon reduced widths be of like magnitude, that the excitation energies be about the same, and that other similar levels be far enough away to avoid confusion.

In the scheme to the left the horizontal bars represent the amplitudes for the neutron or proton dimensionless reduced widths. For the bound states we define the amplitude as the absolute square root of the spectroscopic factor from either $^{16}\text{O}(d, p)$ or $^{16}\text{O}(d, n)$ stripping. The observed spectroscopic factors are about 0.9 for the ground and first excited states of both nuclei^{46, 47} and about 0.03 for the other two bound states in ^{17}O . For an unbound or resonant state the squared amplitude is $\gamma^2/(\hbar^2/\mu r^2)$. For ^{17}O the resonant amplitudes were deduced⁸ for a 3.86-fm radius inside a potential well. For ^{17}F the amplitudes shown for all but levels 29-31 were deduced by Salisbury and Richards^{48, 49} for a 5.1-fm radius. Levels 29-31 are from Prior *et al.*⁴⁵

The figure shows good correspondence for the lengths of the bars for the mirror pairs even

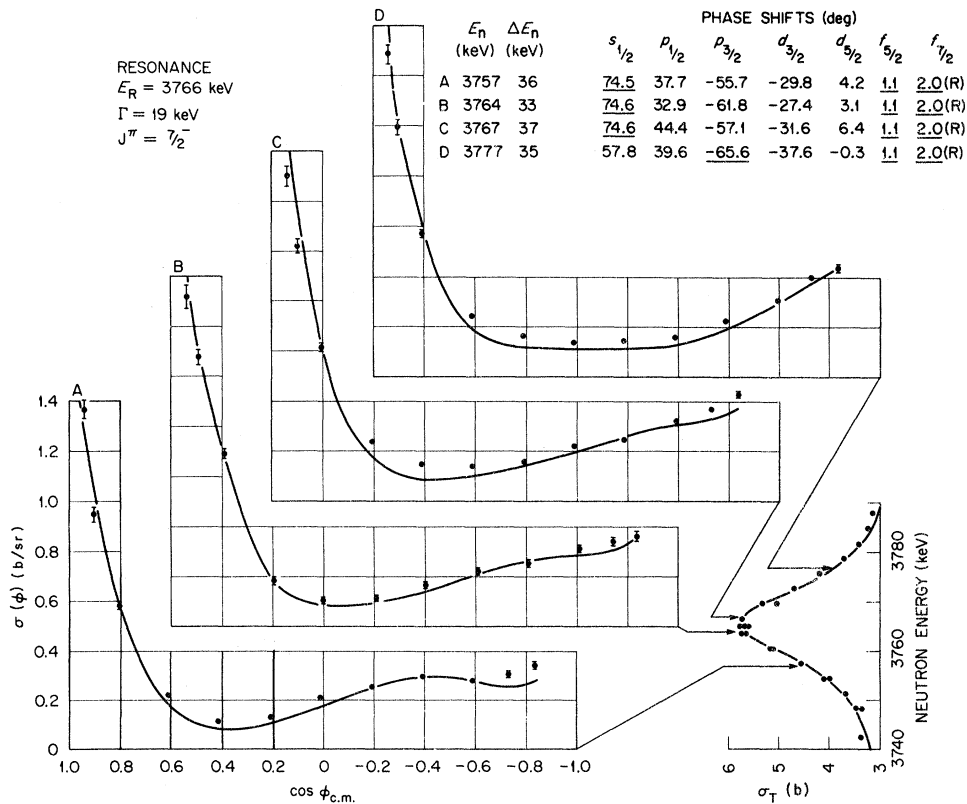


FIG. 10. Least-squares analyses of the scattering distributions of Ref. 2 near the 3.766-MeV, $7/2^-$ resonance. The average neutron energies, energy spreads (full width at half maximum), and phase shifts are listed at the upper right. The underlined phase shifts are fixed at the R -matrix values. For $f_{7/2}$ waves the potential phase shift is $+2^\circ$ and the resonance is included.

though the neutron and proton amplitudes are based on different R -matrix methods and different boundary radii for the two nuclei. An exception is the $\frac{3}{2}^+$ pair near 9 MeV. This pair might not have been considered definite because the reported reduced widths differ by a factor of 10; however, the discrepancy is due mostly to the fact that the ^{17}O width is from a multilevel analysis⁸ whereas the ^{17}F width is not.⁴⁵ Multilevel effects are significant for the $\frac{3}{2}^+$ levels. (The lower $\frac{3}{2}^+$ levels in ^{17}F were evaluated^{48, 49} by a multilevel analysis.)

It is interesting that the pairs below 8 MeV have the same level numbers for both nuclei for all but the broad $\frac{3}{2}^+$ pair. Perhaps future assignment will reveal a close correlation in level numbers for all but the broad levels.

In the right-hand figure the pairs for levels 6 and 9 are most probably mirrors; nevertheless, they are relegated to the right because neither the spins or parities are known. This uncertain status is particularly interesting for pair 6. Salisbury

and Richards⁴⁸ assigned $\frac{1}{2}^+$ for the ^{17}F member. That assignment had also been assumed⁵⁰ for the level in ^{17}O and had become accepted³ in the literature, but the observed peak in the neutron total cross sections shows unambiguously that the ^{17}O level is not $\frac{1}{2}^+$ (see Sec. III A). Now, the $\frac{1}{2}^+$ assignment for the ^{17}F member should be questioned. This question does not insult the integrity of the proton-scattering measurements of Salisbury and Richards because, as they state, "The most difficult region is the peak at $E_p = 5.400$ MeV which was shown to arise from two levels, a moderately narrow $\frac{7}{2}^-$ with a very narrow $\frac{1}{2}^+$ superimposed. The $\frac{1}{2}^+$ is not cleanly resolved and, so, was hard to identify."

The higher levels in the right-hand figure show only hints of mirror structure. Some of the levels are fairly broad and are indicated by heavy lines. A close examination suggests that some J^π assignments may be wrong. Obviously several ^{17}F levels are missing above 8 MeV.

Levels 19 in ^{17}O and 26 in ^{17}F are connected by

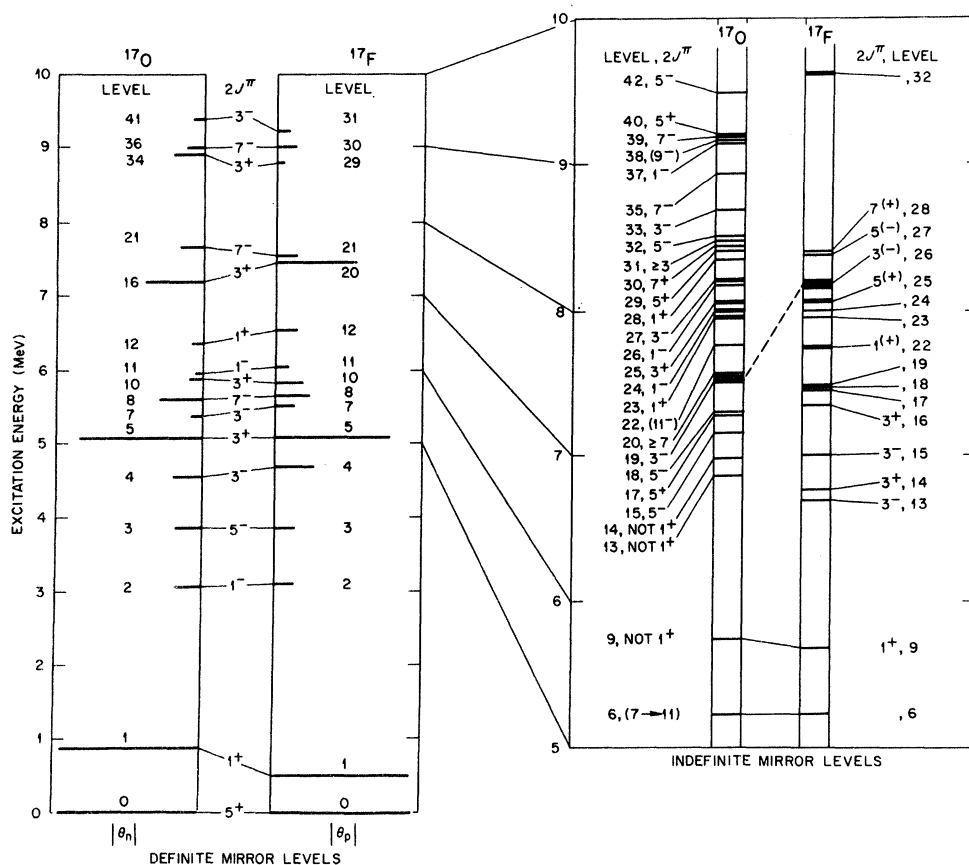


FIG. 11. The ^{17}O and ^{17}F level structures. The ^{17}O levels are from Table III, and the ^{17}F levels are referenced in the text. The left-hand figure includes only levels that appear to be well-established mirrors. The horizontal bar for each member of an established pair represents the reduced width amplitude $|\theta_n|$ or $|\theta_p|$. The remaining levels for both nuclei are relegated to the diagram on the right where the heavy lines indicate broad levels.

a dashed line because both have large widths and $J = \frac{3}{2}$. But the relative parities are unknown. The ^{17}O level is $\frac{3}{2}^-$. Dangle, Oppliger, and Hardie⁵¹ assumed odd parity also for the ^{17}F member and then deduced the parities as indicated for interfering levels 22, 25, 27, and 28. (For levels 29–31 the J^π assignments of Dangle *et al.* disagree with the later work of Prior *et al.*⁴⁵)

VII. CONCLUSION

The experimental level structure in ^{17}O below 9.5 MeV excitation is now relatively well established. There are 43 known states, including the ground state, and 35 of these have known J^π . Some limits can be placed on J^π for each of the other eight states. Most of the excitation energies are known to better than ± 10 keV, and some to ± 2 keV. It seems possible that no more states will ever be found below about 8 MeV. From 8 to 9.5 MeV more levels will probably be discovered but, at the present time, more levels are known in this

region for ^{17}O than for the corresponding region in ^{17}F .

Shell-model calculations are also at an advanced stage. Comparisons⁸ with calculations of Wildenthal and McGrory⁵² show an almost one-to-one correspondence with the observed levels in Table III. These calculations show that most of the levels, except the ground and first excited state and the broad $d_{3/2}$ state at 5.08 MeV, have complicated multiparticle-multihole structures. The near one-to-one correspondence suggests that it is now worthwhile to expend considerable effort to identify the J^π values for the few undetermined levels.

The model calculations of Zuker, Buck, and McGrory⁵³ or of Wildenthal and McGrory⁵² include only the $1p_{1/2}$, $2s_{1/2}$, and $1d_{5/2}$ orbits and give no hint of the expected single-particle strengths of the $\frac{3}{2}^-$, $\frac{3}{2}^+$, $\frac{5}{2}^-$, and $\frac{7}{2}^-$ levels. In the companion paper⁸ the observed reduced widths are deduced for most of the levels by an R -matrix analysis and interpreted in terms of single-particle spectroscopic factors for a combined R -matrix potential-well model.

*Undergraduate student from Auburn University in Oak Ridge National Laboratory Cooperative Educational Program.

†Research sponsored by the U. S. Atomic Energy Commission under contract with Union Carbide Corporation.

¹M.-C. Lemaire, M. C. Mermaz, and K. K. Seth, *Phys. Rev. C* **5**, 328 (1972).

²C. H. Johnson and J. L. Fowler, *Phys. Rev.* **162**, 890 (1967).

³F. Ajzenberg-Selove, *Nucl. Phys.* **A166**, 1 (1971).

⁴W. L. Baker, C. E. Busch, J. A. Keane, and T. R. Donoghue, *Phys. Rev. C* **3**, 494 (1971).

⁵J. L. Fowler and H. O. Cohn, *Phys. Rev.* **109**, 89 (1958).

⁶J. L. Fowler and C. H. Johnson, *Phys. Rev. C* **2**, 124 (1970).

⁷A. M. Lane and R. G. Thomas, *Rev. Mod. Phys.* **30**, 257 (1958).

⁸C. H. Johnson, *Phys. Rev. C* **7**, 561 (1973); erratum submitted to *Phys. Rev.*

⁹M. G. Rusbridge, *Proc. Phys. Soc. Lond.* **A69**, 830 (1956).

¹⁰J. P. Schiffer, A. A. Kraus, Jr., and J. R. Risser, *Phys. Rev.* **105**, 1811 (1957).

¹¹R. B. Walton, J. D. Clement, and F. Boreli, *Phys. Rev.* **107**, 1065 (1957).

¹²B. K. Barnes, T. A. Belote, and J. R. Risser, *Phys. Rev.* **140**, B616 (1965).

¹³G. W. Kerr, J. M. Morris, and J. R. Risser, *Nucl. Phys.* **A110**, 637 (1968).

¹⁴J. K. Bair and F. X. Haas, *Phys. Rev. C* **7**, 1356 (1973).

¹⁵D. B. Fossan, R. L. Walter, W. E. Wilson, and H. H. Barschall, *Phys. Rev.* **123**, 209 (1961).

¹⁶C. H. Johnson and H. E. Banta, *Rev. Sci. Instrum.* **27**, 132 (1956).

¹⁷C. W. Snyder, private communication.

¹⁸R. L. Macklin, private communication.

¹⁹E. H. Beckner, R. L. Bramblett, G. C. Phillips, and T. A. Eastwood, *Phys. Rev.* **123**, 2100 (1961).

²⁰R. O. Bondelid, J. W. Butler, C. A. Kennedy, and A. del Callar, *Phys. Rev.* **120**, 887 (1960).

²¹J. B. Marion, *Rev. Mod. Phys.* **38**, 660 (1966).

²²H. W. Newson, R. M. Williamson, K. W. Jones, J. H. Gibbons, and H. Marshak, *Phys. Rev.* **108**, 1294 (1957).

²³J. H. Gibbons and H. W. Newson, in *Fast Neutron Physics*, edited by J. B. Marion and J. L. Fowler (Interscience, New York, 1960), Pt. I, pp. 133–176.

²⁴R. R. Borchers and C. H. Poppe, *Phys. Rev.* **129**, 2679 (1963).

²⁵*Neutron Cross Sections*, compiled by J. R. Stehn, M. D. Goldberg, B. A. Magurno, and R. Wiener-Chasman, Brookhaven National Laboratory Report No. BNL-325 (U. S. GPO, Washington, D. C., 1966), 2nd ed., 2nd Suppl., Vol. I.

²⁶C. H. Johnson, F. X. Haas, J. L. Fowler, F. D. Martin, R. L. Kernell, and H. O. Cohn, National Bureau of Standards Special Publication No. 299, 1968 (unpublished), Vol. II, p. 851.

²⁷J. L. Fowler, C. H. Johnson, F. X. Haas, and R. M. Feezel, CONF Report No. 710301, 1971 (unpublished), Vol. I, p. 179.

²⁸S. Cierjacks, P. Forti, D. Kopsch, L. Kropp, J. Nebe, and H. Unseld, Kernforschungszentrum Karlsruhe Document No. KFK 1000, 1968 (unpublished).

²⁹A. Okazaki, *Phys. Rev.* **99**, 55 (1955).

³⁰H. R. Striebel, S. E. Darden, and W. Haeberli, *Nucl. Phys.* **6**, 188 (1958).

³¹J. C. Davis and F. T. Noda, *Nucl. Phys.* **A134**, 361 (1969).

³²J. L. Fowler, C. H. Johnson, and F. X. Haas, in *Proceedings of the International Symposium on Nuclear Structure, Contributions, Dubna, 1968* (International

- Atomic Energy Agency, Vienna, Austria, 1968), p. 1
- ³³C. P. Browne, *Phys. Rev.* **108**, 1007 (1957).
- ³⁴R. O. Lane, A. S. Langsdorf, Jr., J. E. Monahan, and A. I. Elwyn, *Ann. Phys. (N.Y.)* **12**, 135 (1961).
- ³⁵L. Galloway, J. L. Fowler, J. A. Harvey, and C. H. Johnson, *Bull. Am. Phys. Soc.* **17**, 442 (1972).
- ³⁶C. K. Bockelman, D. W. Miller, R. K. Adair, and H. H. Barschall, *Phys. Rev.* **84**, 69 (1951).
- ³⁷D. Lister and A. Sayres, *Phys. Rev.* **143**, 745 (1966).
- ³⁸E. Baldinger, P. Huber, and W. G. Proctor, *Helv. Phys. Acta* **25**, 142 (1952).
- ³⁹H. Schölermann, *Z. Phys.* **220**, 211 (1969).
- ⁴⁰T. R. Donoghue, C. E. Busch, J. A. Keane, and H. Paetz gen. Schieck, in *Proceedings of the Third International Conference on Polarization Phenomena in Nuclear Reactions, Madison 1970*, edited by H. H. Barschall and W. Haeberli (Univ. of Wisconsin Press, Madison, Wisconsin, 1971), p. 622.
- ⁴¹R. G. Seyler, in *Proceedings of the Third International Conference on Polarization Phenomena in Nuclear Reactions* (see Ref. 40), p. 624.
- ⁴²D. D. Phillips, in *Angular Distribution in Neutron-Induced Reactions*, compiled by M. D. Goldberg, V. M. May, and J. R. Stehn, Brookhaven National Laboratory Report No. BNL-400 (U. S. GPO, Washington, D. C., 1962), 2nd ed., Vol. I.
- ⁴³H. H. Williams, E. K. Warburton, K. W. Jones, and J. W. Olness, *Phys. Rev.* **144**, 801 (1966).
- ⁴⁴S. T. Thornton, *Phys. Lett.* **39B**, 623 (1972); I. D. Proctor, W. Benenson, and D. L. Bayer, *Bull. Am. Phys. Soc.* **17**, 442 (1972); H. G. Bingham, H. T. Fortune, J. D. Garrett, and R. Middleton, *ibid.* **17**, 921 (1972).
- ⁴⁵R. M. Prior, K. W. Corrigan, E. D. Berners, and S. E. Darden, *Nucl. Phys.* **A167**, 143 (1971).
- ⁴⁶I. M. Naqib and L. L. Green, *Nucl. Phys.* **A112**, 76 (1968).
- ⁴⁷S. T. Thornton, *Nucl. Phys.* **A137**, 531 (1969).
- ⁴⁸S. R. Salisbury and H. T. Richards, *Phys. Rev.* **126**, 2147 (1962).
- ⁴⁹H. T. Richards, private communication.
- ⁵⁰K. Bethge, D. J. Pullen, and R. Middleton, *Phys. Rev. C* **2**, 395 (1970).
- ⁵¹R. L. Dangle, L. D. Oppliger, and G. Hardie, *Phys. Rev.* **133**, B647 (1964).
- ⁵²B. H. Wildenthal and J. B. McGrory, private communication; quoted in Ref. 1.
- ⁵³A. P. Zuker, B. Buck, and J. B. McGrory, *Contributions to the International Conference on Properties of Nuclear States, Montréal, Canada, 1969* (Presses de l'Université de Montréal, Montréal Canada 1969), p. 193.